Paper 10

THE MEASUREMENT OF OIL-FILM THICKNESS IN ELASTOHYDRODYNAMIC CONTACTS

By A. Dyson*, H. Naylor*, and A. R. Wilson*

To assess the validity of elastohydrodynamic lubrication theory, values of oil-film thickness predicted by Dowson and Higginson are compared with measurements obtained by experiment in a disc machine lubricated with a wide variety of fluids. It is shown that, over the range 1–40 μin (micro-inches), theoretical and measured values are in close agreement for most of the fluids examined. Thus, over this range the predicted dependence of film thickness h upon rolling speed u, viscosity η_0, and pressure coefficient of viscosity α is confirmed. The experimental results are consistent with the expression $h \alpha (u\eta_0)^{0\cdot65}\alpha^{0\cdot56}$. The insensitivity of film thickness to load at loads exceeding 400 lb/in and to sliding at constant rolling speed is also demonstrated. A tentative explanation is offered of the discrepancies between theoretical and measured values that emerge under conditions producing thicker films.

Unlike most of the fluids examined, a polymer solution and a polydimethyl silicone fluid formed films significantly thinner than predicted. The possibility that the behaviour of these fluids is affected by their non-Newtonian characteristics is being investigated.

INTRODUCTION

AN EXPRESSION FOR the thickness of the oil film between loaded rotating cylinders that has been derived by Dowson and Higginson (1)† on the basis of elastohydrodynamic theory is:

$$h = 1\cdot6(u\eta_0)^{0\cdot7}\alpha^{0\cdot6}E'^{0\cdot03}R^{0\cdot43}w^{-0\cdot13}$$

Experimental determinations of film thickness by Crook (2), Sibley and Orcutt (3), and Christensen (4) presented in Fig. 10.1‡ show that this expression is substantially correct but that significant differences exist between the slopes of the plots of the experimental results. In an attempt to resolve these differences, measurements of film thickness made in a disc machine with a number of lubricants of widely differing physical properties are compared with values calculated from the expression by Dowson and Higginson.

The MS. of this paper was first received at the Institution on 2nd April 1965 and in its revised form, as accepted by the Council for publication, on 5th May 1965.

* *Shell Research Ltd, Thornton Research Centre, Chester.*

† *References are given in Appendix 10.IV.*

‡ *In constructing Fig. 10.1 the following values of pressure–viscosity coefficient were assumed:*

Crook's oil: $\alpha = 2\cdot6\times10^{-9}$ *cm²/dyne at 40°C*
Christensen's oil: $\alpha = 1\cdot78\times10^{-9}$ *cm²/dyne at 58°C*

Notation

$2b$	Length of Hertzian contact zone.
$\frac{b}{R}$	$= 4\sqrt{(W/2\pi)}$.
C_C	$= C_T - C_M$; electrical capacitance, pF, between two discs separated by a lubricant film.
C_M	Electrical capacitance, pF, measured between the two discs when they are separated by a large air gap. This includes stray capacitances to earth.
C_T	Total electrical capacitance, pF, measured between the two discs when the machine is running.
C'	$= C_i' + C_h' + C_o'$; total electrical capacitance between two discs, e.s.u. cm per cm transverse width, calculated on various assumptions detailed in the text.
C_h'	Electrical capacitance, e.s.u. cm per cm transverse width, between the Hertzian flats of two discs separated by a lubricant film.
C_i'	Electrical capacitance e.s.u. cm per cm transverse width, of the inlet sections of two discs.
C_o'	Electrical capacitance, e.s.u. cm per cm transverse width, of the outlet sections of two discs.

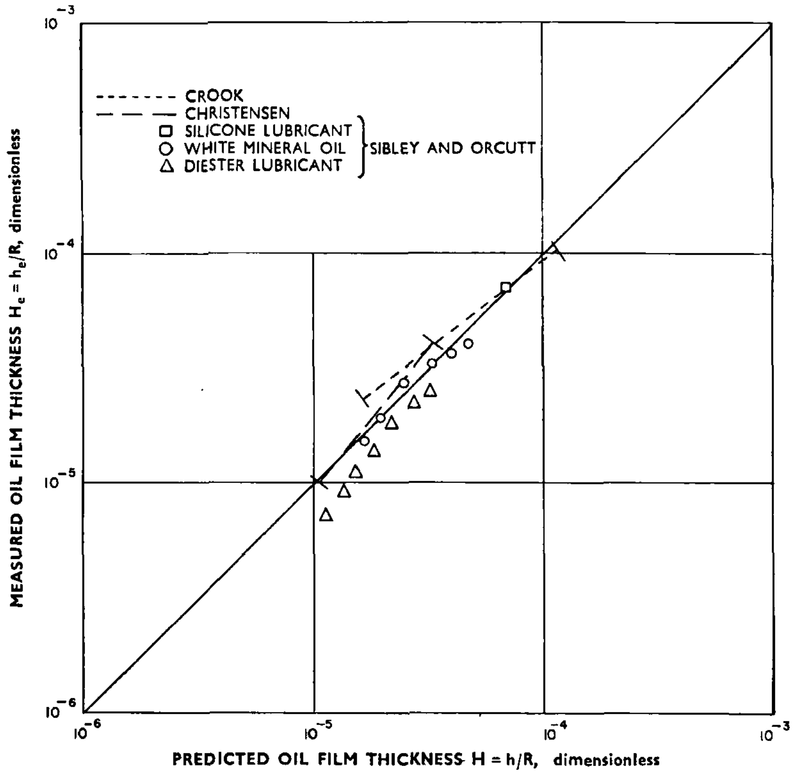

Fig. 10.1. Comparison between measured values of film thickness in rolling previously published and calculated values predicted by Dowson and Higginson

E_1, E_2 Elastic moduli of solids in contact.

E' Reduced elastic modulus, such that

$$\frac{1}{E'} = \frac{1}{2}\left[\frac{1-\sigma_1^2}{E_1} + \frac{1-\sigma_2^2}{E_2}\right].$$

G $\alpha E'$.

H h/R.

H_e h_e/R.

h Predicted lubricant film thickness, cm.

h_e Experimental lubricant film thickness, cm.

h_0 Film thickness on line of centres, cm.

h_0' Thickness, cm, of lubricant film assumed to separate the parallel surfaces of the Hertzian flats on two loaded lubricated elastic discs.

h_1 Lubricant film thickness, cm, between two lightly loaded stationary discs.

h_2 Lubricant film thickness, cm, between two heavily loaded stationary discs.

L Transverse load-bearing width of contact, cm.

p Pressure.

q Reduced pressure, defined by

$$q = \frac{1}{\alpha}(1 - e^{-\alpha p}).$$

R Effective radius of roller pair, defined by

$$R = \frac{R_a R_b}{R_a \pm R_b}.$$

R_a, R_b Radii of cylinders or rollers in contact.

U Dimensionless parameter $= \eta_0 u/E'R$.

u Mean rolling speed $= \frac{1}{2}(u_1 + u_2)$.

u_1, u_2 Surface velocities of solids in x direction.

W Reduced load $= w/E'R$.

w Load per unit width of cylinder.

$X_{o,\,i}$ $= \dfrac{b^2}{2Rh_0'}\dfrac{\epsilon_0}{\epsilon_1}$.

x Co-ordinate in direction of motion.

$Y_{o,\,i}$ $= (\epsilon_0 \epsilon_1 R/h_0')^{-1/2} C_{i,\,o}'$.

α Pressure exponent of viscosity, $\eta = \eta_0 \exp(\alpha p)$.

δ $1 - \zeta$.

ϵ_0 Dielectric constant of lubricant at atmospheric pressure and at the temperature of the disc surfaces.

ϵ_1 $= \epsilon_0$ for inlet section.
$= 1$ for outlet section.

ϵ_h Dielectric constant of lubricant at the temperature of the disc surfaces and at the mean Hertzian pressure in the contact.

ξ $= x/b$.

ζ $= b/x$.

η Viscosity.

η_0 'Controlling viscosity', viscosity at conditions of entry to contact.

σ_1, σ_2 Poisson's ratio.

EXPERIMENTAL

The disc machine

The disc machine used in this investigation was similar in principle to that described by Crook (5). The discs, which were of case-hardened En 34 steel, measured 3 in in diameter and 1 in in width. The reduced elastic modulus E' of this material was taken as $2 \cdot 24 \times 10^{12}$ dyne/cm²; the reduced radius R was 1·905 cm. To accommodate small relative axial displacements of the discs the edges of one disc were radiused, giving an effective contact width of 0·875 in. The dimensionless load parameter $W = w/E'R$ was therefore $4 \cdot 7 \times 10^{-6}$ per 100 lb load between the discs. The discs were ground to an eccentricity less than 0·0001 in and to a surface roughness of 1·5 to 2 μin c.l.a. This finish was finally improved to better than 0·8 μin c.l.a. by polishing with diamond paste.

The discs were electrically insulated from each other so that the thickness of the oil film between them could be derived from measurements of capacitance. In preliminary work each disc was connected to the capacitance bridge through a simple mercury contact, while the temperatures of the discs were indicated by thermocouples trailing lightly on the disc surfaces. From various indications, however, the accuracy of the trailing thermocouples was suspected and to check this another thermocouple was embedded $\frac{1}{8}$ in below the surface of each disc. Compared with the embedded thermocouples the trailing thermocouples indicated temperatures as much as 10 degC too low. Consequently, in the work described in this paper only the embedded thermocouples were used.

Slip-rings were then fitted to connect the thermocouples to a recorder and the discs to the capacitance bridge. Replacement of the mercury contacts by slip-rings did not affect the repeatability of capacitance measurements. However, since the capacitance of the recorder was large and variable a switch was fitted so that the recorder could be disconnected from the live disc whenever a capacitance measurement was made.

To control the temperature of the discs and hence the viscosity of the adhering oil film a supply of test oil was maintained to the sides of the discs as well as to the contact. The oil was pumped through a system of heaters, coolers, and filters and the supply to each disc was adjusted in temperature and quantity to produce the disc temperatures required. This method of control was most effective when used with oils of low viscosity at high temperatures and low speeds and when the discs were in rolling contact. Under the most adverse conditions it proved impossible to maintain constant temperatures and it was then necessary to measure capacitance and temperature alternately and to derive simultaneous values of capacitance and temperature by interpolation.

The discs were normally operated at temperatures which were equal to within 1 degC, but at high sliding speeds differences of up to 5 degC could occur in spite of separate adjustments of the oil supply to each disc. The temperature controlling the viscosity η_0 of the oil in the entry zone was then taken as the arithmetic mean of the temperatures of the two discs.

Measurement of oil-film thickness

Crook (5) deduced oil-film thicknesses from measurements of the electrical capacitance between each disc and a lightly loaded pad riding on the oil film adhering to the surface of that disc. He also used a second method in which he calculated the oil-film thickness from the capacitance between the two discs, and showed that the results given by this method were in essential agreement with those obtained by the first method.

In the work described in this paper, the authors used Crook's second method, i.e. that based on the capacitance between the two discs. To estimate film thicknesses from the capacitance readings, the same assumptions were made as used by Crook, namely:

(1) The shape of the discs is the same as in the Hertzian case of dry contact, but with the addition of a constant separation, h_0'.

(2) The inlet and Hertzian sections are full of oil, but at the outlet section the film divides into two parts, each of thickness $h'_0/2$, one part adhering to each disc. The remainder of the outlet section is composed of air.

With these assumptions, the total capacitance between the discs could be calculated for a series of assumed values of h_0' at a given constant load, and a calibration curve of film thickness against capacitance could thus be established. Further details are given in Appendix 10.I.

The capacitance between the discs was measured with a Wayne Kerr Radio Frequency Bridge type B 601, the bridge output being displayed on an oscilloscope. Difficulty was caused by the frequent bridging of the film by low-resistance contacts, presumably either directly between asperities of the opposing surfaces or through conducting particles trapped between them. These contacts disturbed the bridge balance when their resistance approached the reactance of the condenser. This disturbance was less, the higher the frequency used, but an upper limit to the frequency was set by the condition that the reactance of the disc should be large compared with the total resistance of the leads from the bridge through the slip-rings to the discs.

It was necessary to filter the bridge output to reduce the disturbances caused by the low-resistance contacts, and also to eliminate a cyclic fluctuation at rig speed which was attributed to a slight eccentricity of the discs. The upper frequency limit of the tunable band-pass filters available was 20 kc/s and for this reason the bridge operating frequency was set at 19 kc/s. A block diagram is given in Fig. 10.2.

With this arrangement it was found that the apparent resistance usually remained approximately constant over several cycles. The bridge output at any given time was of the form

$$\Delta C \sin(\omega t + \delta) + \Delta R \cos(\omega t + \delta)$$

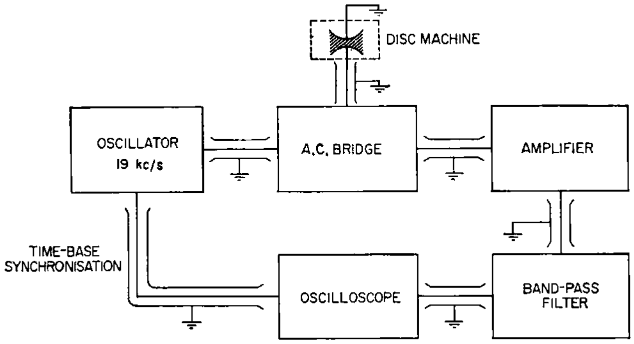

Fig. 10.2. Block diagram of arrangements for measurement of capacitance between discs

where ΔC is a capacity unbalance term, ΔR is a resistance unbalance term, and δ is a phase angle.

At any given capacitance setting, the oscilloscope pattern consisted of a series of sine waves, each corresponding to a different value of ΔR. These sine waves converged in a series of nodal points, corresponding to

$$\omega t+\delta = \frac{(2n+1)\pi}{2}$$

where n is an integer. This is illustrated in Fig. 10.3, where the time base is displayed horizontally and the filtered bridge output vertically.

The relative vertical displacement between successive nodal points, corresponding to odd and even values of n, was therefore proportional to ΔC, and the capacitance balance was obtained when all these nodal points fell on the same horizontal level.

Physical properties of the lubricants

The measurements reported in this paper were obtained with lubricants chosen for their variety in origin and physical properties. These are briefly described below and some physical properties are presented in Appendix 10.II. These properties and the methods by which they were obtained have been discussed more fully by Galvin, Naylor, and Wilson (**6**).

Lubricant	*Description*
A	High viscosity-index mineral oil (predominantly paraffinic)
B	Medium viscosity-index mineral oil to OM100 specification
D	High viscosity, low viscosity-index mineral oil (predominantly aromatic and naphthenic)
F	Low-viscosity-index mineral oil+methacrylate polymer
G	Ethylene oxide–propylene oxide copolymer
I	Castor oil
L	Di(2-ethylhexyl) sebacate
M	Polydimethylsilicone (Midland Silicone Fluid) MS200/1000).

An important physical quantity which enters into the theoretical formula for film thickness is the pressure coefficient of viscosity α. The theory of Dowson and coworkers is a numerical theory in which an exponential viscosity–pressure relation is assumed:

$$\eta = \eta_0 \exp(\alpha p)$$

This relation is only an approximation to the behaviour of most real fluids, and the question arises as to what value of α should be used in the calculation of predicted film thicknesses.

For most of the lubricants the value of α was obtained from the mean slope of the curve of logarithm of viscosity against pressure, over the arbitrarily chosen pressure range 0–5000 lb/in^2. The errors involved are discussed in Appendix 10.III, where it is shown that this procedure is probably acceptable, at any rate for the mineral oils. The greatest errors are likely to arise with di(2-ethylhexyl) sebacate (lubricant L), and here a more accurate value

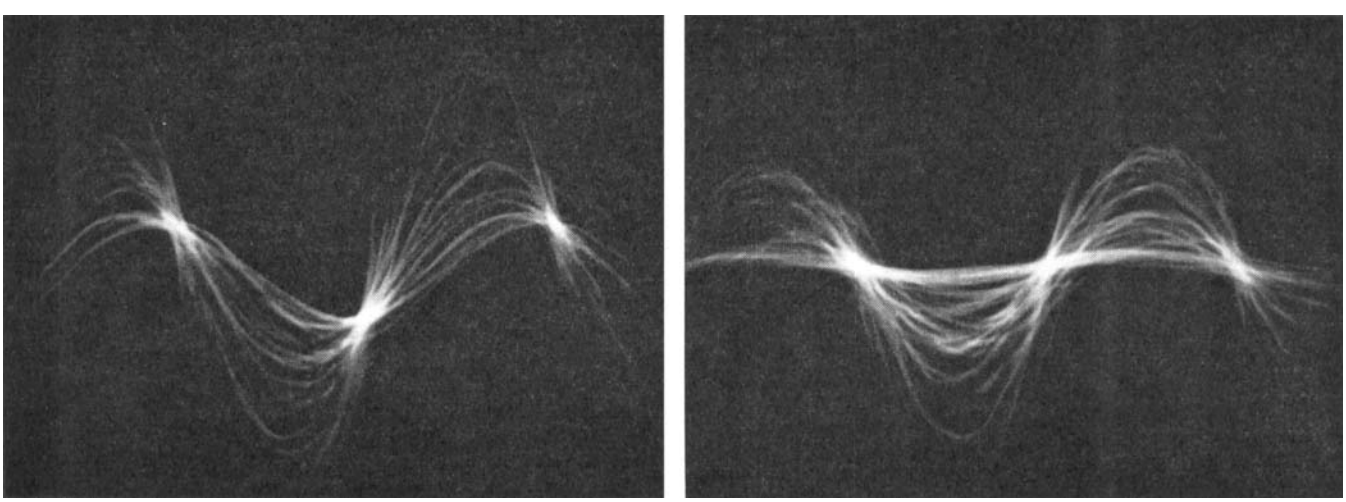

a *b*

Fig. 10.3. Display of bridge output: (a) bridge unbalanced, (b) bridge balanced

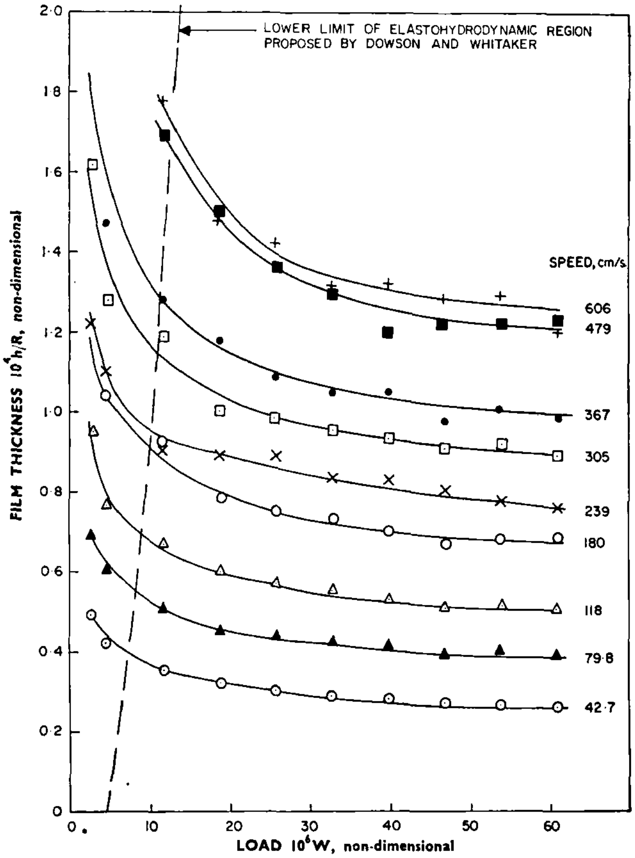

Fig. 10.4. Effect of load on film thickness: lubricant A

was obtained by numerical integration of the data published for this substance by the American Society of Mechanical Engineers (7); further details are given in Appendix 10.III.

RESULTS

Effect of load

The dependence of film thickness on load in rolling contact was investigated with lubricant A at a constant disc surface temperature of 40°C and at speeds between 107 and 1520 rev/min (42·7–606 cm/s rolling speeds).

The variation of film thickness with load at various speeds is shown in Fig. 10.4, which also shows the limit of the elastohydrodynamic regime according to Dowson and Whitaker (8). We should therefore expect that the points corresponding to loads of 286 lb/in ($W = w/E'R = 11{\cdot}7 \times 10^{-6}$) should be on the borderline, and that those corresponding to the seven heaviest loads should conform to the full elastohydrodynamic theory.

In Fig. 10.5 the means of the logarithms of the dimensionless film thicknesses, taken over the nine speeds shown in Fig. 10.4, are plotted against the logarithms of the loads. It appears that the points for the seven heaviest loads fall on a straight line, within experimental error, while that for the load corresponding to $W = 11{\cdot}7 \times 10^{-6}$ lies off this line.

This conclusion is confirmed by a statistical analysis which also shows that the slope of the log–log plot of film thickness against load for the seven heaviest loads does not vary significantly with speed. The mean slope is 0·147

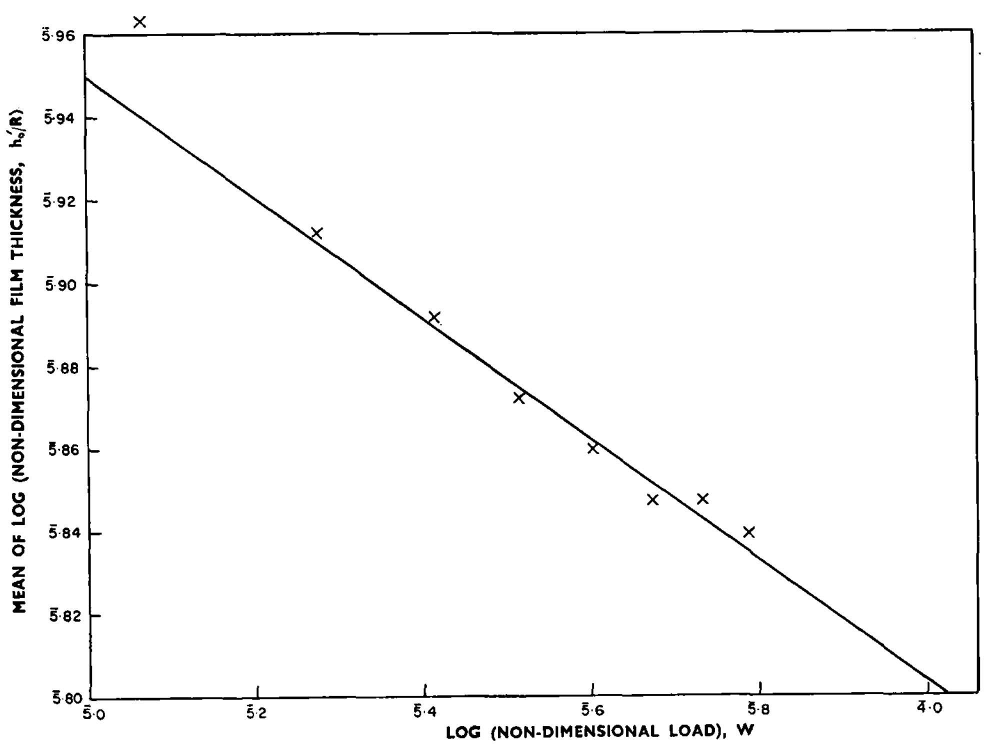

Fig. 10.5. Effect of load (W) on the mean thickness of films of lubricant A at rolling speeds of 42·7 cm/s to 606 cm/s

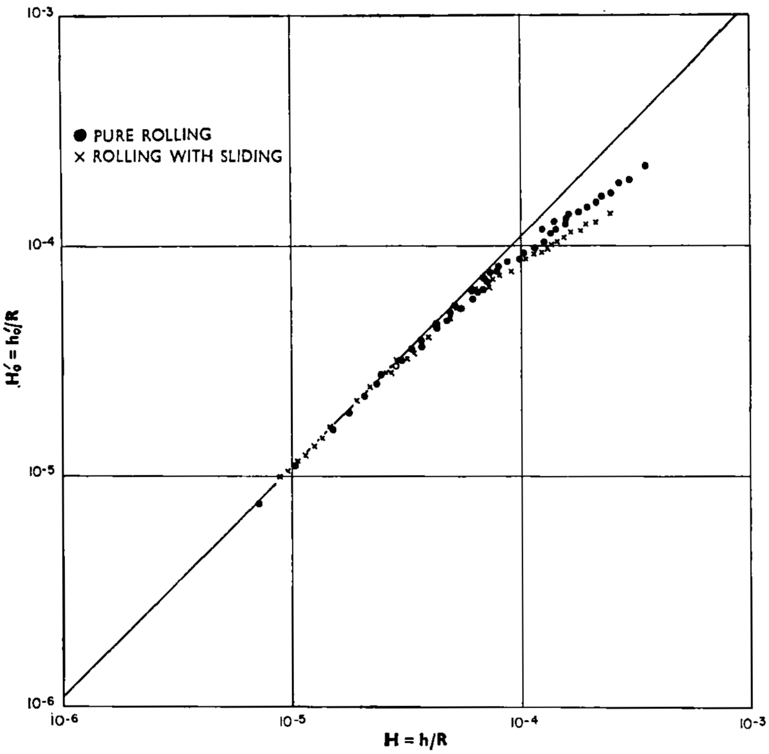

Fig. 10.6. Lubricant A: comparison of measured non-dimensional oil-film thickness $H_0' = h_0'/R$ with predicted values $H = h/R$

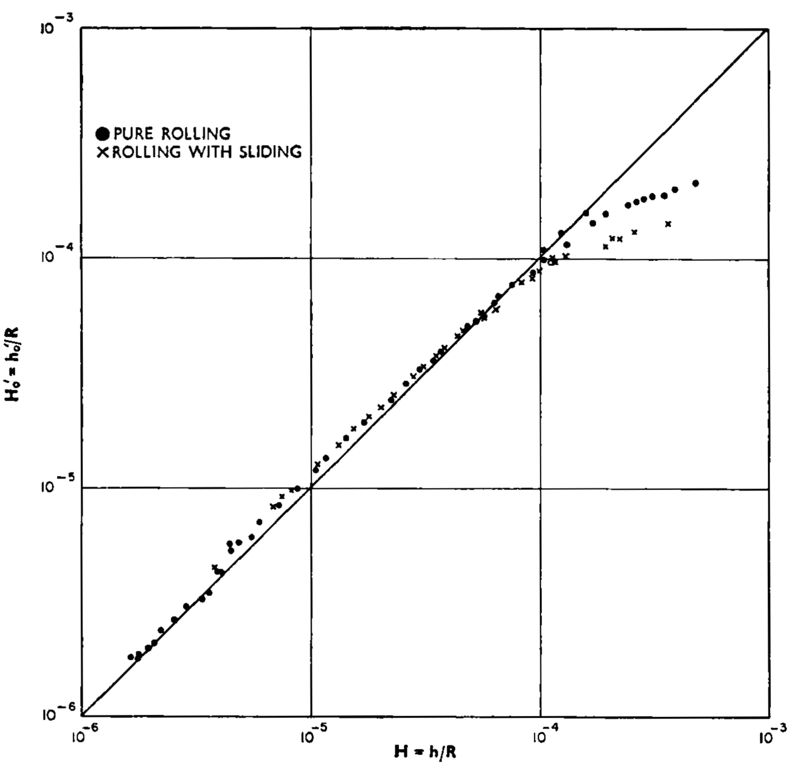

Fig. 10.7. Lubricant B: comparison of measured non-dimensional oil-film thickness $H_0' = h_0'/R$ with predicted values $H = h/R$

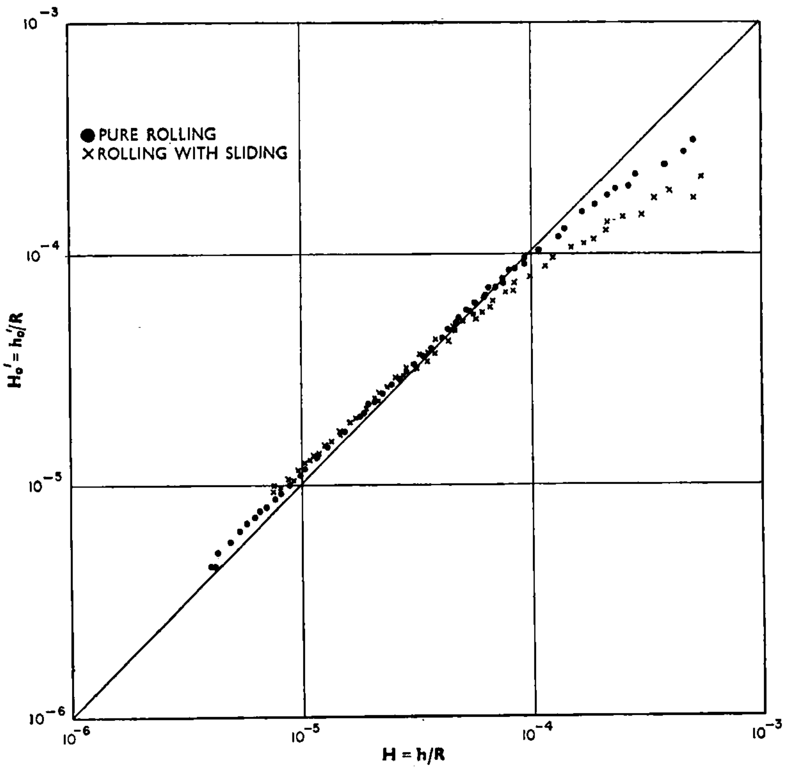

Fig. 10.8. Lubricant D: comparison of measured non-dimensional oil-film thickness $H_0' = h_0'/R$ with predicted values $H = h/R$

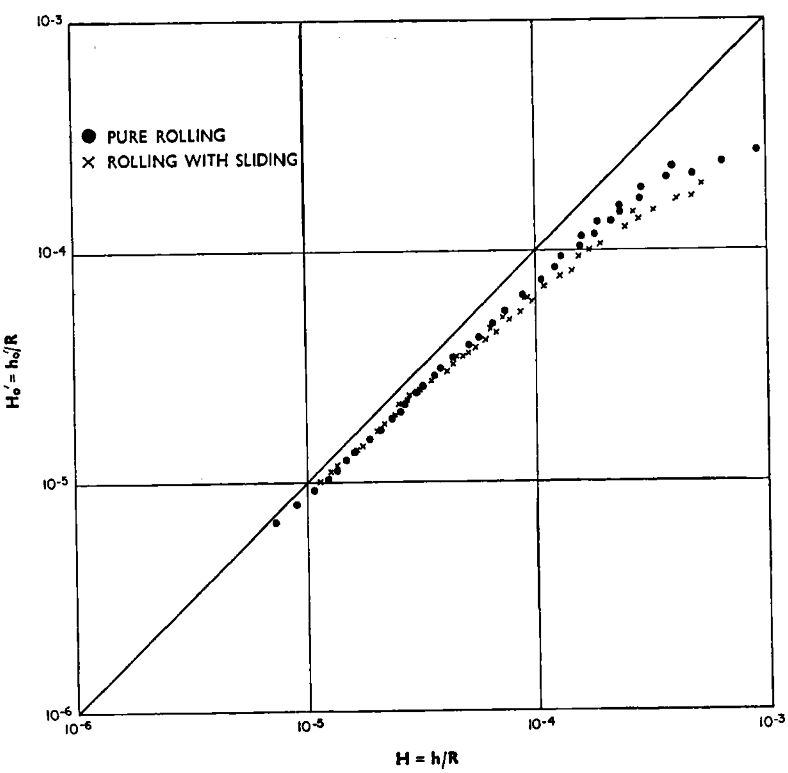

Fig. 10.9. Lubricant F: comparison of measured non-dimensional oil-film thickness $H_0' = h_0'/R$ with predicted values $H = h/R$

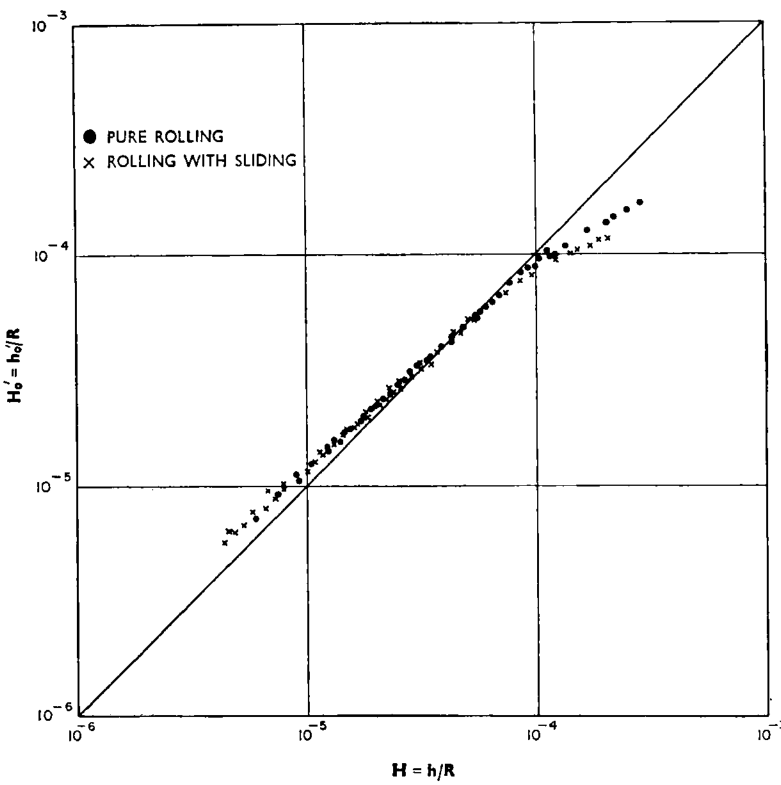

Fig. 10.10. Lubricant G: comparison of measured non-dimensional oil-film thickness $H_0' = h_0'/R$ with predicted values $H = h/R$

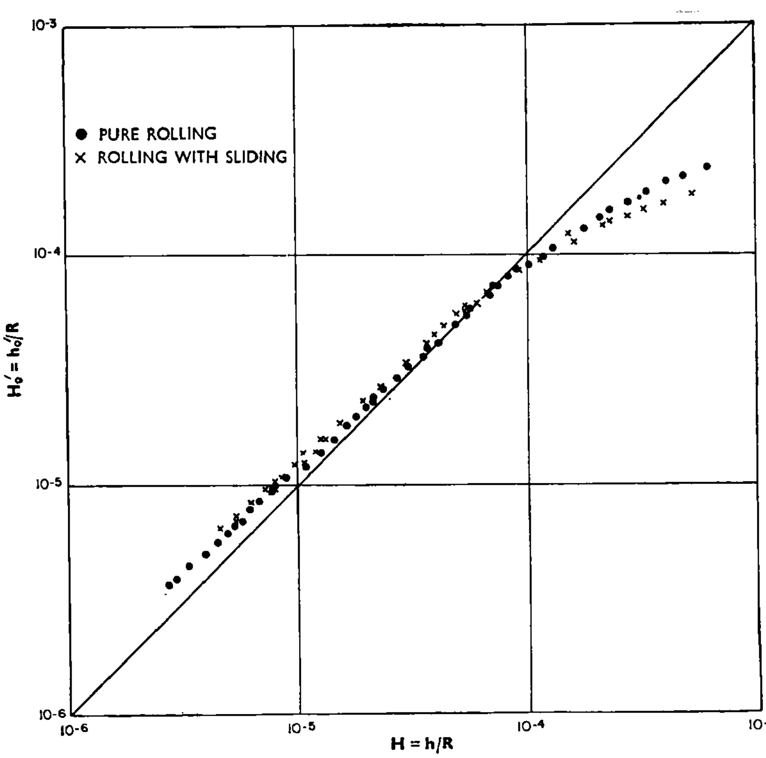

Fig. 10.11. Lubricant I: comparison of measured non-dimensional oil-film thickness $H_0' = h_0'/R$ with predicted values $H = h/R$

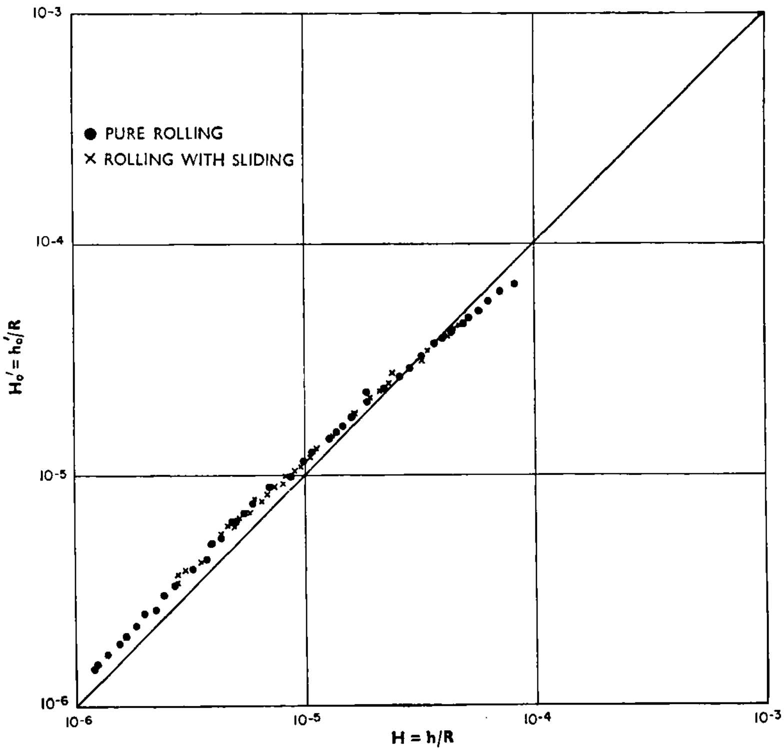

Fig. 10.12. Lubricant L: comparison of measured non-dimensional oil-film thickness $H_0' = h_0'/R$ with predicted values $H = h/R$

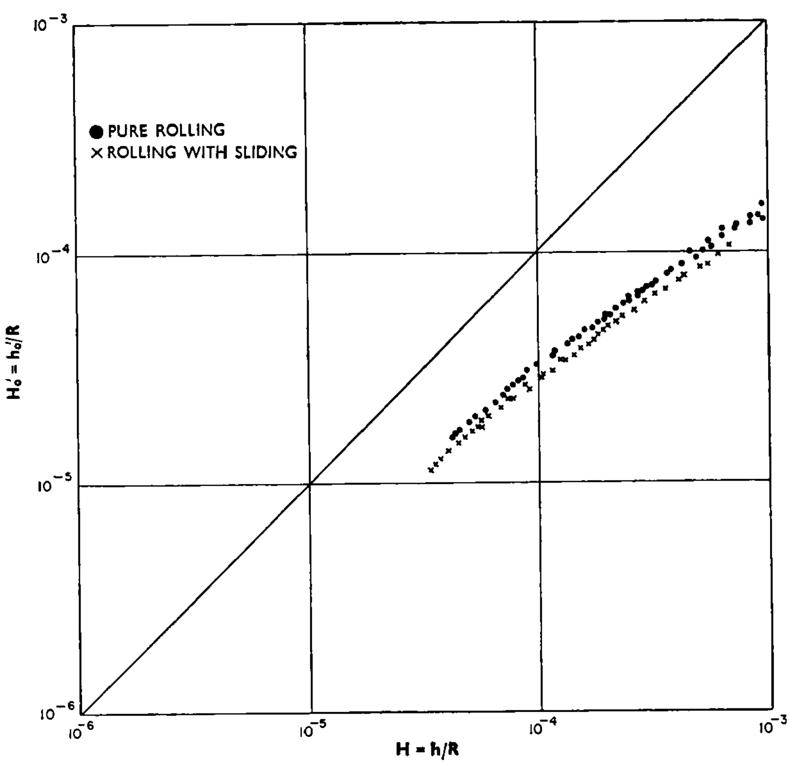

Fig. 10.13. Lubricant M: comparison of measured non-dimensional oil-film thickness $H_0' = h_0'/R$ with predicted values $H = h/R$

with 95 per cent confidence limits $\pm 0{\cdot}013$. The Dowson and Higginson value of 0·13 therefore lies just outside these limits, but there may well be systematic errors of such a magnitude as to bring it within the limits. The 95 per cent confidence limits of a single observation of film thickness are approximately ± 4 per cent, calculated from the scatter of the observations about the regression lines. This figure is well within what would be regarded as acceptable in view of the many assumptions and approximations involved in the experimental determinations and their interpretation in terms of film thickness.

Effect of speed and viscosity

In experiments to determine the dependence of film thickness on rolling speed and viscosity, the choice of the load to be applied between the discs was limited by two opposing considerations. To ensure elastohydrodynamic conditions in the contact the load had to be greater than that corresponding to $W = 11{\cdot}7 \times 10^{-6}$. The effect of increasing load, however, was to extend the Hertzian contact area and so impair measurements of capacitance by increasing the frequency of electrical contact between the discs. For these reasons a load of 625 lb/in was adopted; the corresponding value of W was $25{\cdot}8 \times 10^{-6}$.

Although the minimum oil-film thickness which could be measured in sliding was limited by the frequency of bridging, this limit was not encountered in pure rolling. For the thinnest film so far measured in pure rolling, $h_0'/R = 0{\cdot}62 \times 10^{-6}$ ($h_0' = 0{\cdot}45$ μin or approximately 100 Å); this value, obtained with lubricant B, is in reasonable agreement with the value of $H = 0{\cdot}5 \times 10^{-6}$ predicted by Dowson and Higginson for the conditions under which this measurement was made ($u = 8{\cdot}0$ cm/s, $\eta = 0{\cdot}036$ poise at 135°C, $\alpha = 1{\cdot}52 \times 10^{-9}$ cm²/dyne, and $W = 25{\cdot}8 \times 10^{-6}$).

The upper limit of film thickness in both rolling and in rolling with sliding was determined by the tendency of the temperature of the discs to rise with increasing rolling speed. Any attempt to increase film thickness by increasing speed was offset by a compensating decrease in viscosity with increasing temperature, the product of speed and viscosity remaining approximately constant.

Within these upper and lower limits measurements were made of the thickness of films formed by eight fluids over the range governed by the viscosities of the individual lubricants. When the discs were in rolling contact they were coupled by gears of 1:1 ratio, whereas in rolling with sliding a set of 3:1 ratio was used. In this condition the sliding speed $(u_2 - u_1)$ was equal to the mean rolling speed $\frac{1}{2}(u_1 + u_2)$ In Figs 10.6–10.13 measurements made both in rolling and in rolling with sliding are plotted in dimensionless form against values calculated from the expression proposed by Dowson and Higginson.

DISCUSSION

The main conclusion derived from the work described is that for six of the eight lubricants tested, dimensionless film thicknesses measured within the range 10^{-6} to 5×10^{-5} (approximately 1–40 μin or 0·025–1 μ) agree well with those predicted by the theoretical expression of Dowson and Higginson. This is true both for pure rolling and for rolling with sliding, and the agreement seems to be rather closer than that reported by other authors.

The Dowson and Higginson theoretical expression is

$$\frac{h}{R} \propto (u\eta_0)^{0\cdot 7}\alpha^{0\cdot 6}w^{-0\cdot 13}$$

and the following experimental relations have been proposed:

Sibley and Orcutt	$\frac{h_e}{R} \propto (u\eta_0\alpha)^{0\cdot 75}w^{-0\cdot 36}$
Crook	$\frac{h_e}{R} \propto (u\eta_0)^{0\cdot 5}$
Christensen	$\frac{h_e}{R} \propto (u\eta_0)^{0\cdot 83}w^{-0\cdot 2}$

In the work described, the slopes of the experimental lines were in general rather less than that suggested by theory. Describing the results obtained by a proportionality relationship between h_e/R and the Dowson and Higginson expression raised to some power, and including the load dependence that has been established for lubricant A, the following expression was obtained:

$$h_e/R \propto (u\eta_0)^{0\cdot 65}\alpha^{0\cdot 56}w^{-0\cdot 15}$$

This expression is valid for lubricants A, B, D, G, I, and L over the range in which each adheres most closely to the Dowson and Higginson line. Each of the six lubricants shows a falling away from the theoretical line at dimensionless film thicknesses greater than about 5×10^{-5}, and this will be discussed below. Lubricant B is of special interest since it is a sample of the oil used by Crook. In an effort to understand the discrepancies between the results obtained and those of Crook, several measurements were made at the frequency used by Crook, 1 kc/s, but these fitted in with the other results at 19 kc/s. The authors are still unable to explain these discrepancies.

In many cases the measured film thicknesses are somewhat greater than the theoretical values, but these latter are the minimum film thicknesses h_{min} at the outlet constriction (Fig. 10.14). The mean film thicknesses over the Hertzian region should correspond more closely to the constant separation h_0' between the Hertzian flats which have been assumed for the interpretation of the

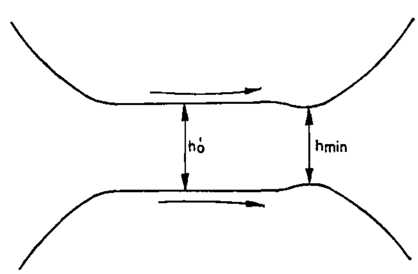

Fig. 10.14. Sketch of typical elastohydrodynamic contact

capacitance measurements in terms of film thicknesses. These mean film thicknesses should be approximately 14 per cent greater than the minimum thicknesses (**9**), but there are other factors which would be expected to reduce the experimental estimates. These are the close approach of asperities of one surface to those of the other surface, and the thinning of the lubricant film at the sides owing to side leakage. The effect of these factors cannot be estimated with any degree of precision, and the final outcome of these considerations is the acceptance of experimental film thicknesses up to 14 per cent greater than the theoretical values.

Many of the values recorded in Figs 10.6–10.13 exceed this limit, and this may be the result of errors in the interpretation of the capacitance measurements in terms of film thicknesses. However, the model of the contact geometry assumed for the interpretation of the results should approach more closely to the true geometry at the smaller film thicknesses.

It is easy to advance plausible reasons for the finding of experimental film thicknesses smaller than the theoretical values, but a discrepancy in the opposite sense is more difficult to explain. Since the effect is apparent in pure rolling as well as in rolling with sliding, it cannot be the result of hydrodynamic action of the sliding asperities. Other possibilities are the squeeze effect between asperities approaching each other in the inlet region, and the normal stress differences owing to the viscoelasticity of the lubricant.

In contrast with the six fluids discussed above, lubricants F (a solution of a polymer in a mineral oil) and M (a polydimethyl silicone) formed films significantly thinner than predicted over the whole range of measurement. Similar behaviour of silicones in a crossed-cylinders machine has been reported by Archard and Kirk (**10**). Since the Dowson and Higginson theory assumes Newtonian behaviour of the lubricant, and since lubricants such as F and M are known to depart from Newtonian behaviour under conditions which are mild compared with those expected to occur in the inlet region of the disc machine, the authors tentatively attribute the results obtained with these two fluids to non-Newtonian behaviour. The authors are currently investigating this aspect in greater detail.

With the six other lubricants discussed above, the dimensionless film thicknesses agree well with the Dowson and Higginson predictions up to about 5×10^{-5}, beyond which the measured values become progressively less than predicted. The divergence is more marked when sliding is present, and it is therefore unlikely to be the result of emergence of non-Newtonian behaviour in these lubricants, since sliding makes very little difference to the film thicknesses of the non-Newtonian lubricants F and M.

Furthermore, it is unlikely to be the result of heating of the oil by adiabatic compression in the inlet zone, since this too would not be affected by sliding. The most likely explanation of the discrepancies in film thickness with thicker films is probably that the lubricant is heated by shear in the inlet region; this would be expected to increase in importance when sliding is introduced.

ACKNOWLEDGEMENTS

The authors would like to thank Mr W. J. Cairney for assistance in developing the disc machine and for making most of the experimental measurements, Professor H. Blok for drawing attention to the problem of the value of α to be used, and Mr A. G. Green for the computation of the capacities of the inlet and outlet sections given in Table 10.1.

APPENDIX 10.1

CALCULATION OF FILM THICKNESS FROM CAPACITANCE BETWEEN DISCS

The geometry of the discs near their conjunction is shown in Fig. 10.15. In Fig. 10.15*a* the discs are assumed to be stationary under a very light load, insufficient to cause elastic deformation. They are in contact along a line, the intersection of which with a plane normal to the axes of rotation is taken as the origin O of the x co-ordinate, in the direction of peripheral motion. The space between the discs is assumed to be filled with oil. The oil-film thickness h for small values of x is given by

$$h_1 \simeq \frac{x^2}{2R} \quad . \quad . \quad . \quad . \quad . \quad (10.1)$$

where R is the radius of relative curvature, i.e. if R_a and R_b are the radii of the discs

$$\frac{1}{R} = \left[\frac{1}{R_a}+\frac{1}{R_b}\right]$$

In Fig. 10.15*b* a normal load has been applied to the discs, which

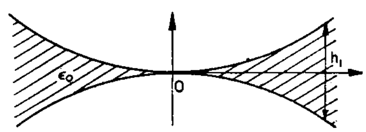

(a) Discs stationary under light load

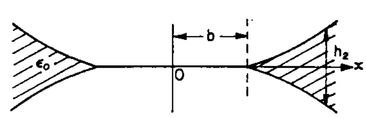

(b) Discs stationary under heavy load

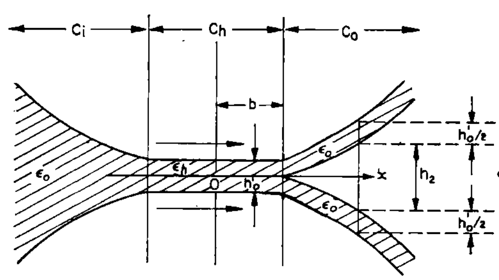

(c) Discs in motion under heavy load

Fig. 10.15. Geometry of discs near conjunction between them

are still stationary. This is a special case of the classical problem of Hertz. The line of contact is broadened into a band of width $2b$, where

$$b = 2\left[\frac{2}{\pi} w \frac{R}{E'}\right]^{1/2} \quad . \quad . \quad . \quad . \quad (10.2)$$

where w is the load per unit transverse width and E' is the reduced modulus which is given by

$$\frac{2}{E'} = \frac{1-\sigma_1^2}{E_1} + \frac{1-\sigma_2^2}{E_2}$$

where σ_1, σ_2 and E_1, E_2 are respectively the Poisson's ratio (< 1) and the Young's modulus of the materials of the two contacting discs.

The shape of the gap between the two cylinders outside the band of contact is given by

$$h_2 = \frac{b^2}{2R}\{|\xi\sqrt{(\xi^2-1)}| - \ln[|\xi| + |\sqrt{(\xi^2-1)}|]\} \quad (10.3)$$

where $\xi = x/b \geqslant 1$. As $b \to 0$, $h_2 \to h_1$, as given by equation (10.1).

Fig. 10.15c shows the configuration assumed when the discs are in motion under a heavy load. The surfaces are assumed to have the same shape as in Fig. 10.15c, with the addition at all points of a constant film thickness h_0'. Thus the separation between the two surfaces inside the Hertzian contact band is assumed to be h_0', and outside this band $(h_0'+h_2)$. This procedure seems plausible since the value of h_0' is normally small compared with the maximum elastic deflections of the surfaces. Furthermore, such an assumed shape approximates quite well to those computed by Dowson, Higginson, and Whitaker (9).

The inlet section and the Hertzian contact region are assumed to be completely filled with oil. At the junction of the Hertzian region and the outlet section it is assumed that the oil film separates into two films, each of thickness $h_0'/2$, and each adhering to the surface of a disc. The remaining part of the section, of thickness h_2, is assumed to be air.

Given b and h_0' it is desired to compute the total capacitance C' between the two discs in units of e.s.u. of capacity cm per cm transverse width. The total capacitance is divided into three sections:

$$C' = C_i' + C_h' + C_o' \quad . \quad . \quad . \quad . \quad (10.4)$$

where C_i' is the capacitance (cm/cm) of the inlet region, C_h' the capacitance (cm/cm) of the Hertzian region, and C_o' the capacitance (cm/cm) of the outlet region.

The capacitance C_h' of the Hertzian region may be set down immediately as

$$C_h' = \frac{\epsilon_h b}{2\pi h_0'} \quad . \quad . \quad . \quad . \quad . \quad (10.5)$$

where ϵ_h is the dielectric constant of the oil in the Hertzian region. It is normally estimated at the mean surface temperature of the discs and at the mean Hertzian pressure in the contact. The capacitance of the inlet or outlet region is given by

$$C_{i,o}' = \int_{\pm b}^{\pm\infty} \frac{dx}{[4\pi(h_0'/\epsilon_0 + h_2/\epsilon_1)]} \quad . \quad . \quad (10.6)$$

where ϵ_0 is the dielectric constant of the oil at the mean surface temperature of the discs and at atmospheric pressure. For the inlet film, ϵ_1 will be put equal to ϵ_0; and for the outlet film, $\epsilon_1 = 1$. In general, ϵ_0 will differ from ϵ_h owing to the effect of pressure on the dielectric constant.

Substituting for h_2 from equation (10.3), the following is obtained from equation (10.6):

$$C_{i,o}' = \frac{\epsilon_0 b}{4\pi h_0'}\int_1^\infty \frac{d\xi}{1+X\{|\xi\sqrt{(\xi^2-1)}| - \ln[|\xi| + |\sqrt{(\xi^2-1)}|]\}}$$

where $$X \equiv \frac{b^2}{2Rh_0'}\frac{\epsilon_0}{\epsilon_1}$$

To avoid the infinity in the limits the variable is changed to

$$\zeta = \frac{1}{\xi}$$

thus giving

$$Y = \frac{2^{1/2}}{4\pi} X^{1/2} \int_0^1 \frac{d\zeta}{\zeta^2 + X\{|\sqrt{(1-\zeta^2)}| - \zeta^2 \ln[|1/\zeta| + |\sqrt{(1/\zeta^2-1)}|]\}} \quad . \quad . \quad . \quad (10.7)$$

where $$Y = (\epsilon_0\epsilon_1 R/h_0')^{-1/2} C_{i,o}'$$

The asymptotic limits of this integral may be calculated without difficulty. As $X \to 0$, $b \to 0$ and $h_2 \to h_1$. Substituting for h_1 from equation (10.2) into equation (10.6) gives

$$C_{i,o}' = \frac{\epsilon_1 R}{2\pi}\int_0^\infty \frac{dx}{(2Rh_0'\epsilon_1/\epsilon_0)+x^2} = \frac{\epsilon_1 R}{2\pi}\left(\frac{\epsilon_0}{2Rh_0'\epsilon_1}\right)^{1/2}\frac{\pi}{2}$$

or

$$Y = \frac{1}{4\sqrt{2}} = 0{\cdot}1768 \quad (X \to 0) \quad . \quad . \quad (10.8)$$

As $X \to \infty$, the range of ζ over which there is an appreciable contribution to the integral shrinks to a small region near $\zeta = 1$. Thus

$$\zeta = 1 - \delta$$

and $$|\sqrt{(1-\zeta^2)}| - \zeta^2 \ln\left[\frac{1}{\zeta} + |\sqrt{(1/\zeta^2-1)}|\right] \simeq \frac{4\sqrt{2}}{3}\delta^{3/2}$$

plus higher powers of δ.

Table 10.1. Relation between Y and X

$$X = \frac{b^2}{2Rh_0'}\frac{\epsilon_0}{\epsilon_1}$$

$$Y = \frac{(2X)^{1/2}}{4\pi}\int_0^1 \frac{d\zeta}{\zeta^2 + X\{|\sqrt{(1-\zeta^2)}| - \zeta^2 \ln[|1/\zeta| + |\sqrt{(1/\zeta^2-1)}|]\}}$$

Entries in the table are the values of Y for selected values of X given by the product of row and column headings. Precision is estimated as 1 part in 10^3.

	10^{-3}	10^{-2}	10^{-1}	1	10	10^2	10^3
1	0·1735	0·1678	0·1548	0·1324	0·104 2	0·076 78	0·054 41
1·5	0·1729	0·1661	0·1515	0·1277	0·099 11	0·072 42	0·051 08
2	0·1723	0·1648	0·1490	0·1242	0·095 56	0·069 42	0·048 83
3	0·1714	0·1627	0·1452	0·1193	0·090 64	0·065 38	0·045 80
4	0·1707	0·1610	0·1424	0·1157	0·087 21	0·062 61	0·043 75
5	0·1701	0·1597	0·1400	0·1129	0·084 60	0·060 52	0·042 22
6	0·1695	0·1585	0·1381	0·1106	0·082 50	0·058 87	
7	0·1690	0·1574	0·1364	0·1087	0·080 74	0·057 01	
8	0·1686	0·1565	0·1349	0·1070	0·079 25	0·056 32	
9	0·1682	0·1556	0·1336	0·1055	0·077 94	0·055 31	

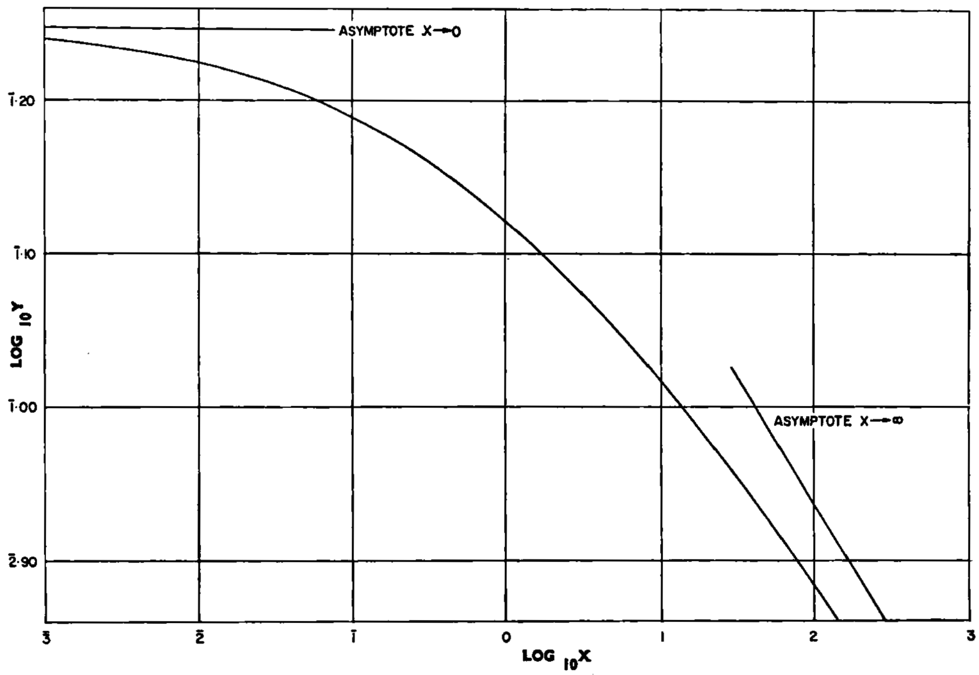

Fig. 10.16. Relation between Y and X used in determination of capacitance of inlet and outlet sections

The integral to be evaluated is therefore

$$\int_0^1 \frac{d\delta}{1+\frac{4\sqrt{2}}{3}X\delta^{3/2}}$$

putting

$$\frac{4\sqrt{2}}{3}X\delta^{3/2} = \tan^2\theta; \qquad \frac{d\delta}{d\theta} = \frac{4}{3}\left(\frac{3}{4\sqrt{2}X}\right)^{2/3}(\tan\theta)^{1/3}\sec^2\theta$$

gives

$$\int_0^1 \frac{d\delta}{1+\frac{4\sqrt{2}}{3}X\delta^{3/2}} = \left(\frac{2}{3X^2}\right)^{1/3}\int_0^1 (\tan\theta)^{1/3}\, d\theta$$

This integral may readily be evaluated numerically. Near $\theta = \pi/2$ the variable must be changed to

$$\phi = \frac{\pi}{2}-\theta$$

and

$$\int_{\pi/2-\beta}^{\pi/2}(\tan\theta)^{1/3}\,d\theta = \int_0^\beta \phi^{-1/3}\,d\phi = \frac{3}{2}\beta^{2/3}$$

where β is a small angle, such that

$$\tan\beta \simeq \beta$$

It is found that $\int_0^1 (\tan\theta)^{1/3}\,d\theta \simeq 1{\cdot}81$

and

$$Y = \frac{2^{1/2}}{4\pi}X^{1/2}\left(\frac{2}{3}\right)^{1/3}X^{-2/3}(1{\cdot}81)$$

$$= 0{\cdot}186X^{-1/6} \quad (X\to\infty) \quad . \quad . \quad . \quad (10.9)$$

The function given by equation (10.7) was integrated numerically by a digital computer for values of X ranging from 10^{-3} to 5×10^3, and the results are presented in Table 10.1 and plotted in Fig. 10.16. To obtain the relation between film thickness h_0' and total capacitance C' between the discs for any given load and disc geometry, b is first calculated from equation (10.2). Then a series of values are assumed for h_0 and C_h' is calculated from equation (10.5) and C_i', C_o' from equation (10.7) and Fig. 10.16. For the inlet section,

$$X_i = \frac{b^2}{2Rh_0'}$$

and for the outlet section

$$X_o = \frac{b^2\epsilon_o}{2Rh_0'}$$

where $\epsilon_1 = 1$.

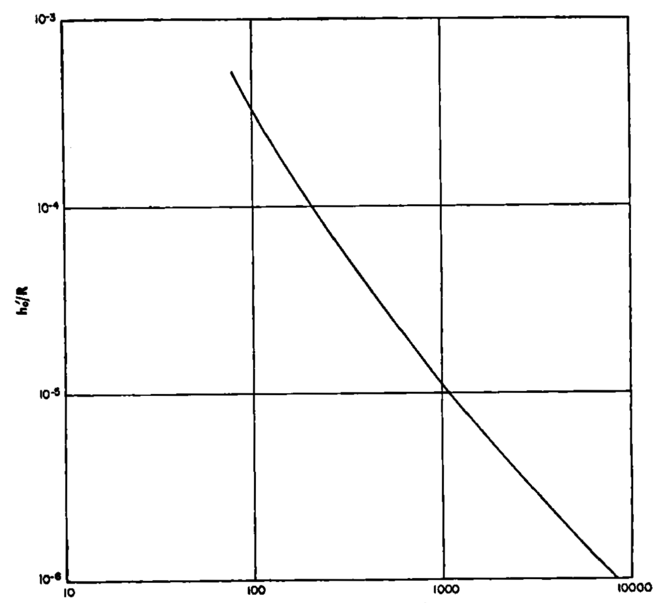

Fig. 10.17. Calibration curve for lubricant A relating film thickness h_0'/R to the calculated capacitance between the discs C_c

Equation (10.4) then gives the total capacitance C' between the discs in e.s.u. cm per cm transverse width. This is converted into the capacitance C_c obtained in picofarads from the experimental observations by the relation

$$C_c = LC'/0{\cdot}9$$

where L is the transverse width in centimetres.

A calibration curve may be plotted in the form of a graph of the quantity C_c against the assumed values of the film thickness h_0'. This calibration curve varies slightly with temperature, and in practice the authors have calculated curves for temperatures of 40°C and 80°C. Capacitances measured at other disc temperatures are subjected to a small correction based on linear interpolation or extrapolation. The dielectric constants are measured at 20°C and 100°C, and the estimates at 40°C and 80°C are made by linear interpolation. The dielectric constant ϵ_h in the Hertzian region is similarly estimated from the measurements made at various temperatures and pressures.

An example of a calibration curve of C_c against h_0' is given in Fig. 10.17. A separate calibration is required for each value of the load.

The experimental determination of the capacitance C_c between the discs is made as follows. The total measured capacitance C_T includes the effect of stray capacitances to earth from the unshielded disc, shaft, and force-measuring equipment. These stray effects are defined by the capacitance C_M, approximately 250 pF, measured when the discs are separated by a large air gap. The theoretical capacitance between the discs under these conditions, 2–3 pF, is usually within the error of the bridge measurement, and is ignored. Thus the capacitance between the discs is

$$C_c = C_T - C_M$$

APPENDIX 10.II

PHYSICAL PROPERTIES OF LUBRICANTS USED

Some physical properties of the lubricants are given in Tables 10.2–10.4.

Table 10.2. General viscosity and density data

Lubricant	Kinematic viscosity, cS, at		Kinematic viscosity index	Specific gravity, 60°/60°F	Specific gravity, relative to water at 60°F, at		
	100°F	210°F			30°C	60°C	100°C
A	175·3	15·36	96	0·891	0·884	0·866	0·843
B	83·0	8·8	84	0·899	0·890	0·872	0·851
D	180·1	10·84	8	0·946	0·938	0·920	0·895
F	219·8	17·73	99	0·944	0·931	0·915	0·890
G	143·4	24·10	142	1·018	1·008	0·983	0·955
I	295	20·2	87	0·963	0·955	0·935	0·909
L	12·58	3·31	153	0·918	0·908	0·887	0·859
M	767·4	306·5	—	0·978	0·965	0·941	0·907

Table 10.3. The effect of pressure on the viscosity of lubricants

Lubricant	Gauge pressure, lb/in²	Absolute viscosity, poise, at			Pressure coefficient α (cm²/dyne) $\times 10^{-9}$ between 0 and 5000 lb/in², at		
		30°C	60°C	100°C	30°C	60°C	100°C
A	0	2·50	0·505	0·126	2·5	2·13	1·76
	5000	5·90	1·05	0·232			
B	0	1·22	0·263	0·073	2·70	2·16	1·75
	5000	3·10	0·555	0·135			
D	0	3·10	0·442	0·094	3·46	2·63	1·95
	5000	10·25	1·10	0·185			
F	0	1·73*	0·60	0·153	3·10	2·44	1·85
	5000	4·60*	1·39	0·290			
G	0	2·04	0·625	0·225	1·76	1·43	1·22
	5000	3·80	1·04	0·350			
I	0	2·46*	0·80	0·180	1·59	1·44	1·23
	5000	4·18*	1·31	0·274			
L	0	0·149	0·0621	0·0282	1·50	1·29	1·16
	5000	0·249	0·097	0·0421			
M	0	8·70	5·01	2·73	1·81†	1·92†	2·02†

* Measured at 40°C.

† These values were calculated from results reported by Boelhouwer and Toneman (11); they correspond with measurements of viscosity at pressures of 0 and 400 bars.

Table 10.4. Dielectric constants of lubricants at 19 kc/s

Lubricant	Temperature, °C	Dielectric constant at	
		0 lb/in²	50 000 lb/in²
A	20	2·29	2·42
	100	2·18	2·37
B	20	2·33	2·46
	100	2·19	2·39
D	20	2·58	2·53
	100	2·41	2·63
F	20	2·57	2·53
	100	2·41	2·62
G	20	5·85	6·91
	100	4·74	6·01
I	20	4·71	5·28
	100	3·89	4·48
L	20	4·02	4·44
	100	3·41	3·92
M	20	2·77	3·22
	100	2·51	3·02

APPENDIX 10.III

THE VALUE OF THE PRESSURE COEFFICIENT OF VISCOSITY

In this paper, the authors compare measured values of the thickness of the lubricant film in an elastohydrodynamic contact with predicted values. The predicted values are based on the theory of Dowson and co-workers (1) (8) (9), a numerical theory in which it is assumed that there is an exponential relation between viscosity and pressure:

$$\eta = \eta_0 \exp(\alpha p) \quad . \quad . \quad . \quad . \quad (10.10)$$

Most lubricants obey this law approximately, but there are important deviations from it, and it is necessary to enquire whether these deviations can be taken into account in the predicted values of film thickness. Although the theory of Dowson *et al.* is confined to the simple exponential viscosity–pressure law (equation (10.10)), alternative relations may be accommodated in approximate film thickness theories, such as that of Grubin (12). In theories of this type, the shape of the gap between the two discs is assumed, and conditions are sought in which the hydrodynamic pressure at the inlet side of the Hertzian zone tends to infinity. The hydrodynamics of the system are governed by the integrated form of the Reynolds equation:

$$\frac{\mathrm{d}p}{\mathrm{d}x} = 12\eta u(h-h_m)/h^3 \quad . \quad . \quad . \quad (10.11)$$

where $u = \frac{1}{2}(u_1+u_2)$, u_1 and u_2 being the peripheral velocities of the discs, and h_m is the film thickness at the point where $\mathrm{d}p/\mathrm{d}x = 0$.

If η is a function of p, equation (10.11) may be integrated (13) to give:

$$\int \frac{\eta_0}{\eta(p)}\,\mathrm{d}p = \int 12\eta_0 u(h-h_m)\,\mathrm{d}x/h^3 = q \qquad (10.12)$$

where q is the pressure which would have been obtained with an isoviscous lubricant, for which $\eta(p) = \eta_0$ for all pressures. This pressure q may be obtained from the well-known classical theory of hydrodynamics.

Substituting for $\eta_0/\eta(p)$ in equation (10.12) from equation (10.10) and integrating over the pressure limits from zero to p the conventional definition of q as the 'reduced pressure' is obtained:

$$\frac{1}{\alpha}(1-\mathrm{e}^{-\alpha p}) = q$$

If, further, p is allowed to tend to infinity,

$$\frac{1}{\alpha} = q_i \quad . \quad . \quad . \quad . \quad . \quad . \quad (10.13)$$

where q_i is the value of q at the inlet side of the Hertzian zone. This procedure may be used for any other relation between viscosity and pressure, e.g.

$$\eta(p) = \eta_0(1+p/k)^n \quad . \quad . \quad . \quad (10.14)$$

where k and n are disposable constants. This describes the behaviour of many fluids more accurately than does equation (10.12). Substitution of equation (10.14) into equation (10.12) and integration between the limits $p = 0$ and $p = \infty$ gives

$$\frac{k}{n-1} = q_i$$

Comparison with equation (10.13) then suggests that the quantity α in a Grubin-type theory for a lubricant obeying equation (10.10) should be replaced by another quantity α^* for a lubricant obeying equation (10.14), where

$$\alpha^* = \frac{n-1}{k} \quad . \quad . \quad . \quad . \quad (10.15)$$

Since the Grubin theory for a lubricant obeying equation (10.10) gives predicted film thicknesses agreeing reasonably well with those given by the theory of Dowson and Higginson, it would seem reasonable to use equation (10.15) to give an approximate solution to a theory of the type of Dowson and Higginson for a lubricant obeying equation (10.14).

The viscosity data for most of the lubricants were obtained from reference (6) and are limited to pressures of 15 000 lb/in² and below. In these circumstances, the best course seems to be to fit an expression of the form of equation (10.14) to the data, and to assume that this relation adequately describes the viscosities at higher pressures. The constants were fitted by assuming a series of values of k, and then working out the regression of $\log_{10}$ (viscosity) on $\log_{10}(1+p/k)$, the regression coefficient giving a value of n for each assumed value of k. That value of k was chosen which gave the minimum residual sum of squares in the regression, and the value α^* was then calculated from equation (10.15). In Table 10.5 the results of this process are given for the HVI mineral oil, lubricant A, at the highest temperature, 100°C, and for the MVI mineral oil, lubricant B, at the lowest temperature, 30°C. These are likely to give respectively the greatest and the least deviations from equation (10.10) over the whole range of conditions for mineral oils. They are compared with the values α_1 obtained from the mean slope of the curve of the logarithm of viscosity against pressure, taken over the arbitrary pressure range 0–5000 lb/in². The maximum error in the value of α_1 compared with that of α^* is approximately 7·5 per cent, and the corresponding error in the predicted film thickness is 4·5 per cent. In view of the other errors and uncertainties involved in the estimation of film thicknesses from the electrical measurements, the lack of information at pressures above 15 000 lb/in² and the approximate nature of the correction itself, the authors have used the value α_1, as defined above, for α in all predictions of the film thickness from the theory of Dowson and Higginson. The variation of α_1 with temperature was plotted on a graph, and the required values at the different temperatures were obtained by graphical interpolation.

There is one set of results not subjected to the above procedure, namely those obtained with di(2-ethylhexyl) sebacate as a lubricant. Extensive data on the viscosity of this substance as a function of

Table 10.5. Comparison of different estimates of α

Lubricant	Temperature, °C	α^*, dyne^{-1}cm^2	α_1, dyne^{-1}cm^2
A	100	$1{\cdot}63\times10^{-9}$	$1{\cdot}76\times10^{-9}$
B	30	$2{\cdot}62\times10^{-9}$	$2{\cdot}70\times10^{-9}$

Table 10.6. Comparison of estimates of pressure coefficient of viscosity of di(2-ethylhexyl) sebacate obtained by different methods

Temperature, °F	Estimates of pressure coefficient of viscosity, units of 10^{-9} dyne^{-1}cm^2		
	α_1 0–5000 lb/in^2	α_2 numerical integration	α_3 0–120 000 lb/in^2
32	1·78[a]	1·58	1·23[b]
77	1·53	1·27	1·01
100	1·43	1·27	0·92
210	1·06[a]	0·90	0·65
425	0·99[a]	0·68	0·47

[a] Pressure interval 0–10 000 lb/in^2.
[b] Pressure interval 0–107 000 lb/in^2.

pressure have been published by the American Society of Mechanical Engineers (7). These agreed well with the authors' own viscosity measurements up to 15 000 lb/in^2 and it was therefore decided to estimate α on the basis of the A.S.M.E. data. Since the viscosities are given at a large number of pressures, with approximately equal intervals, the left-hand side of equation (10.12) may be integrated numerically, and this is far less time-consuming than the least squares fitting procedure described above. Furthermore, no assumptions as to the form of the viscosity–pressure relation are made.

Suppose the viscosities η_1 and η_2 are known at two pressures p_1 and p_2, where the difference $|p_2-p_1|$ is reasonably small. Then over this small interval it is assumed that the viscosity is given by an exponential relation of the form

$$\eta = \eta_0' \exp(\alpha' p)$$

where η_0' and α' are allowed to be different for different pressure intervals. The contribution to the integral on the left-hand side of equation (10.12), arising from the interval p_1 to p_2, is

$$\begin{aligned}\int_{p_1}^{p_2} \frac{\eta_0}{\eta_0'} \exp(-\alpha' p)\,dp &= \frac{\eta_0}{\eta_0'} \frac{\exp(-\alpha' p_1) - \exp(-\alpha' p_2)}{\alpha'} \\ &= \left(\frac{\eta_0}{\eta_1} - \frac{\eta_0}{\eta_2}\right) \frac{(p_2-p_1)}{\ln(\eta_2/\eta_1)} \\ &= -\frac{\Delta(\eta_0/\eta)\,\Delta p}{\Delta \ln(\eta_0/\eta)}\end{aligned}$$

where the symbol Δ has the usual meaning of a difference.

The integration may be extended to infinite pressure by taking an approximate value of

$$\frac{\Delta p}{\Delta \ln(\eta_0/\eta)}$$

multiplying by the value of (η_0/η) corresponding to the highest pressure recorded, and adding this contribution to the total. This last term to infinity usually forms a very small correction to the total. The reciprocal of the total sum then gives an estimate α_2 of the pressure coefficient of viscosity to be used in the prediction of lubricant film thickness. In Table 10.6, the values α_2 obtained in this way are compared with the values α_1 obtained in the manner previously shown, from the slope of the curve of the logarithm of viscosity against pressure over the range 0–5000 lb/in^2. They are also compared with the estimates α_3 obtained from the mean slope of this curve over the range 0–120 000 lb/in^2 as used by Sibley and Orcutt (3).

The discrepancies between the three sets of estimates are quite high, but di(2-ethylhexyl) sebacate is one of the lowest viscosity lubricants used, and in general, the thinner the lubricant, the greater the divergence from the simple exponential viscosity–pressure relation, equation (10.10), and therefore the greater the discrepancy between the different estimates of α.

APPENDIX 10.IV

REFERENCES

(1) Dowson, D. and Higginson, G. R. 'New roller-bearing lubrication formula', *Engineering, Lond.* 1961 **192,** 158.
(2) Crook, A. W. 'The lubrication of rollers. II—Film thickness with relation to viscosity and speed', *Phil. Trans. Roy., Soc., Series A* 1961 **254,** 223.
(3) Sibley, L. B. and Orcutt, F. K. 'Elastohydrodynamic lubrication of rolling-contact surfaces', *Trans. Amer. Soc. lubric. Engrs* 1961 **4,** 234.
(4) Christensen, H. 'The variation of film thickness in highly loaded contacts', *Trans. Amer. Soc. lubric. Engrs* 1964 **7,** 219.
(5) Crook, A. W. 'The lubrication of rollers—I', *Phil. Trans. Roy. Soc., Series A* 1958 **250,** 387.
(6) Galvin, G. D., Naylor, H., and Wilson, A. R. 'The effect of pressure and temperature on some properties of fluids of importance in elastohydrodynamic lubrication', *Second Lubrication and Wear Convention* May 1964 (Instn Mech. Engrs, London).
(7) American Society of Mechanical Engineers *Pressure–viscosity report* Vol. II 1953.
(8) Dowson, D. and Whitaker, A. V. 'The isothermal lubrication of cylinders', *A.S.L.E.–A.S.M.E. Lubrication Conference* (Washington, D.C.) 1964 (Oct. 13–16).
(9) Dowson, D., Higginson, G. R. and Whitaker, A. V. 'Elastohydrodynamic lubrication: a survey of isothermal solutions', *J. mech. Engng Sci.* 1962 **4** (No. 2), 121.
(10) Archard, J. F. and Kirk, M. T. 'Film thickness for a range of lubricants under severe stress', *Research Notes, J. mech. Engng Sci.* 1964 **6** (No. 1), 101.
(11) Boelhouwer, J. W. M. and Toneman, L. H. 'Viscosity–pressure dependence of some organic liquids', *Proc. Conf. Lubrication and Wear* 1957, 214 (Instn Mech. Engrs, London).
(12) Grubin, A. N. 'Fundamentals of the hydrodynamic theory of heavily loaded cylindrical surfaces', *Symposium on Investigation into the contact of machine components* (Central Scientific Institute for Technology and Mechanical Engineering, Moscow) 1949, Book No. 30 (*D.S.I.R Trans.* No. 337).
(13) Blok, H. 'Inverse problems in hydrodynamic lubrication and design directives for flexible rubbing surfaces', *Proc. International Symposium on Lubrication and Wear* (University of Houston, Texas) 1963.